

Improved Performance of a DFIG Based Wind Power Systems by Using Fuzzy Logic Controller

Subash Muduli

M.Tech Student

Department of Electrical & Electronics Engineering,
Malla Reddy Engineering College,
Ranga Reddy (Dt), Telangana, India.

Mr. P.Ganesh

Assistant Professor

Department of Electrical & Electronics Engineering,
Malla Reddy Engineering College,
Ranga Reddy (Dt), Telangana, India.

Abstract

This paper presents the performance comparison of fuzzy logic controlled wind power systems based on two different induction generators wind turbine simulator for the maximum power extraction. The two induction machines studied for the comparison are the squirrel-cage induction generator (SCIG) and the doubly fed induction generator (DFIG). The techniques of direct grid integration, independent power control, and the droop phenomenon of distribution line are studied and compared between the SCIG and DFIG systems with fuzzy. Both systems are modeled in MATLAB/SIMULINK environment, and the operation is tested for the wind turbine maximum power extraction algorithm results.

Index Terms—Doubly fed induction machines, field-oriented control, Fuzzy logic controller, wind power system.

I. INTRODUCTION

Wind energy is an important source of electrical energy in years to come. Its main advantages come from the fact of being a renewable and environmental-friendly energy. At the beginning it was cheap and very robust but the generated power quality was poor. Most of wind power installations were limited to a few hundred kilowatts connected to distribution grids [1]. Wind turbines and farms grew in size and ratio from the few hundred kilowatts to megawatts size. The increased rated power of wind farms to areas with good wind resources leads to a new problem approach – to which extent the wind power interferes to the power system.

The increasing emphasis on renewable wind energy has given rise to augmented attention on more reliable and advantageous electrical generator systems. Induction generator systems have been widely used and studied in wind power system because of their advantages over synchronous generators, such as smaller size, lower cost and lower requirement of maintenance [1], [2]. The straightforward power conversion technique using squirrel cage induction generator (SCIG) is widely accepted in fixed speed applications with less emphasis on the high efficiency and control of power flow. However, such direct connection with grid would allow the speed to vary in a very narrow range and thus limit the wind turbine utilization and power output. Another major problem with SCIG power system is the source of reactive power; that is, an external reactive power compensator is required to hold the distribution line voltage and prevent the whole system from overload. On the other hand, the doubly fed induction generator (DFIG) with variable-speed ability has higher energy capture efficiency and improved power quality and thus has attracted more attentions. With the advent of power electronic techniques, a back-to-back converter, which consists of two bidirectional converters and a dc link, acts as an optimal operation tracking interface between generator and grid [3]–[5]. Field-oriented control (FOC) is applied to both rotor- and stator-side converters to achieve desirable control on voltage and power [6], [7]. Generally, the FOC has been presented based on DFIG mathematical equations only. However, a three-phase choke is commonly used to couple the stator-side converter into the grid. Therefore, this paper proposes the FOC schemes of

stator-side converter involving the choke, and it turns out that both stator- and rotor side converter voltages consist of a current regulation part and a cross-coupling part.

First, this paper presents a simulation setup to emulate the wind turbine operation in torque control mode and thus to obtain a power operation curve for optimal power control. Second, the modeling and simulation of SCIG and DFIG wind systems are studied. Comparison between SCIG without static Var compensator (STATCOM) and SCIG with STATCOM as well as DFIG system with fuzzy controller is clearly indicates difference in resulted distribution line voltage.

II.MODELING OF WINDTURBINE

Wind energy is extracted through wind turbine blades and then transferred by the gearbox and rotor hub to the mechanical energy in the shaft, which drives the generator to convert the mechanical energy to electrical energy.

$$P_m = C_p(\lambda, \beta) \cdot \frac{1}{2} \rho A v_w^3 \quad (1)$$

where P_m is the mechanical output power in watts, which depends on power performance coefficient C_p , air density ρ , turbine swept area A , and wind speed v_w . $(1/2) \cdot \rho A v_w^3$ is equal kinetic energy contained in the wind at a particular speed v_w . The performance coefficient $C_p(\lambda, \beta)$, which depends on tip speed ratio λ and blade pitch angle β , determines how much of the wind kinetic energy can be captured by the wind turbine system. A nonlinear model describes $C_p(\lambda, \beta)$

$$C_p(\lambda, \beta) = c_1(c_2 - c_3\beta - c_4\beta^2 - c_5)e^{-c_6} \quad (2)$$

Where R_{blade} and ω_r are the blade radius and angular frequency of rotational turbine as depicted in Fig. 1. The $C_p-\lambda$ curve for this particular turbine model at different β is shown in Fig. 2 where it is illustrated that, to achieve maximum C_p , one has $\beta = 0^\circ$ and $\lambda = 8$. The blade with fixed geometry will have fixed $C_p-\lambda$ characteristics, as described in (2) and (3).

Therefore, to track the optimal output power, the curve of $P_m - \omega_r$ is the “map” to follow.

In order to experimentally investigate the operation of wind turbine, a wind turbine emulator system is built to operate in torque control mode, using (1)

$$T = \frac{P}{\omega_r} = \frac{1}{2} \rho \pi R_{blade}^3 v_w^2 \frac{C_p}{\lambda} = \frac{1}{2} \rho \pi R_{blade}^3 v_w^2 C_m \quad (3)$$

Where C_m is the torque performance coefficient. It is dependent on ω_r , v_w , and β . Thus, based on turbine $C_p-\lambda$ model and by assuming $\beta = 0^\circ$, the $C_m-\lambda$ curve is given in Fig. 3. At any particular v_w , one could obtain different torque and, thus, power output by varying rotor speed. The system configuration is shown in Fig. 4, where the ω_r is fed back to the controller for calculating C_m and, then, torque command.

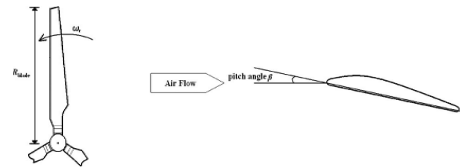


Fig. 1. Schematics of turbine blade from different views.

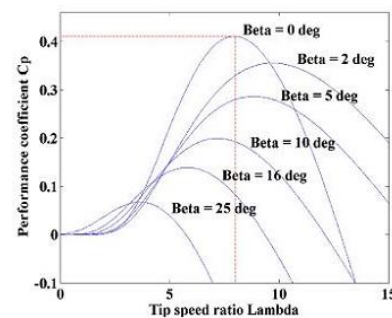


Fig:2. curve for the turbine model

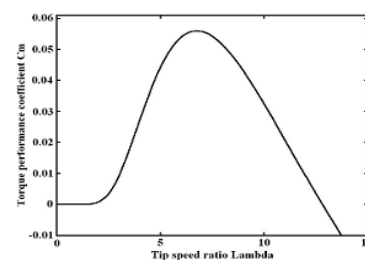


Fig.3. $C_m-\lambda$ curve for the turbine emulator

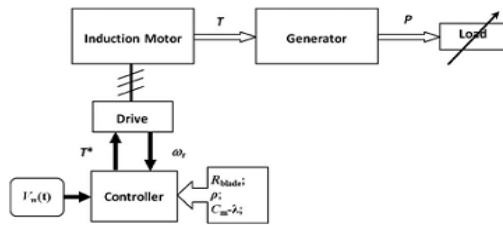


Fig. 4. Wind turbine emulator system

III. DESCRIPTION OF SCIG

The schematics of the SCIG system Fig. 5 shows including the wind turbine, pitch control, and reactive power compensator. The entire system includes three stages for delivering the energy from wind turbine to the power grid. The first one is wind farm stage which handles with low voltage V_{wt} , the second is distribution stage which has medium voltage V_{dis} , and the third is grid transmission stage which has high voltage V_{grid} . The three-phase transformers take care of the interface between stages [9]. As mentioned, nominal power P_{nSCIG} is considered as active power reference to regulate the pitch angle while V_{dis} and I_{dis} denote the distribution line-to-line voltage and phase current, and they are monitored to favor the reactive power compensation for distribution line. This fairly straightforward technique was first used since it is simple and has rugged construction, reliable operation, and low cost. However, the fixed-speed essential and potential voltage instability problems severely limit the operations of wind turbine [1], [3]. Since SCIG is of fixed-speed generator, for a particular wind speed, the output active power is fixed as well. Thus, with the increase of wind speed, so does the output power until the nominal power is reached. The wind speed at this moment is called nominal wind speed so does the output power until the nominal power is reached. The wind speed at this moment is called nominal wind speed. Beyond this speed, the pitch angle system will prevent the output power from exceeding the nominal value. That is, when the wind speed is below nominal value, the power capture can vary with the change of wind speed; and when the wind speed is above nominal value, the pitch angle control system will limit the generated power by changing the pitch angle. In

such way, the output power will be stabilized at nominal value where the wind speed is always above nominal speed. The pitch angle is determined by an open loop control of regulated output active power and by that shown in Fig. 6. Due to the huge size of blade and, thus, inertia, pitch angle has to change in a slow rate and a reasonable range. It is also worthy to notice that, without reactive power source, in Section V, the SCIG system tends to lead to a voltage drop in distribution line which will cause overload problem. In the simulation section, the comparison between SCIG system with and without STATCOM is conducted.

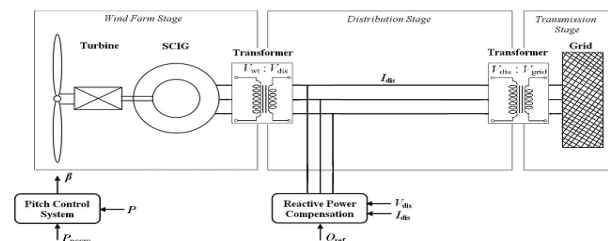


Fig. 5. SCIG wind power system topology

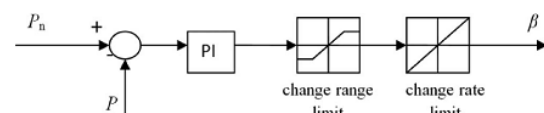


Fig. 6. Pitch angle control

IV. DFIG WIND POWER SYSTEM

Traditionally, the dynamic slip control is employed to fulfill the variable-speed operation in wind turbine system, in which the rotor windings are connected to variable resistor and control the slip by the varied resistance [3], [10]. This type of system can achieve limited variations of generator speed, but external reactive power source is still necessary. Consequently, to completely remove the reactive power compensation and to control both active and reactive power independently, DFIG wind power system is one of most popular methods in wind energy applications [1], [3], [7]. This paper reproduces DFIG model first of all and then concentrates on the controlling schemes of power converters, in which the active and reactive power are controlled independently. In particular, the

stator-side converter control involving an RL series choke is proposed.

Both controlling of rotor- and stator-side converter voltages end up with a current regulation part and a cross-coupling part.

The wind turbine driving DFIG wind power system consists of a wound-rotor induction generator and an ac/dc/ac insulated gate bipolar transistor (IGBT)-based pulse width-modulated (PWM) converter (back-to-back converter with capacitor dc link), as shown in Fig. 7. In this configuration, the back-to-back converter consists of two parts: the stator-/grid-side converter and the rotor-side converter. Both are voltage source converters using IGBTs, while a capacitor between two converters acts as a dc voltage source. The generator stator windings are connected directly to grid (with fixed voltage and frequency of grid) while the rotor winding is fed by rotor-side converter through slip rings and brushes, at variable frequency.

The control system is divided into two parts—stator-side converter control system and rotor-side converter control system. An equivalent circuit of DFIG is depicted in Fig. 8, and the relation equations for voltage V , current I , flux Ψ , and torque T_e are:

$$\begin{aligned} V_{ds} &= R_s I_{ds} - \omega_s \Psi_{qs} + \frac{d\Psi_{ds}}{dt} \\ V_{qs} &= R_s I_{qs} + \omega_s \Psi_{ds} + \frac{d\Psi_{qs}}{dt} \quad (4) \\ V_{dr} &= R_r I_{dr} - s\omega_s \Psi_{qr} + \frac{d\Psi_{dr}}{dt} \\ V_{qr} &= R_r I_{qr} + s\omega_s \Psi_{dr} + \frac{d\Psi_{qr}}{dt} \quad (5) \end{aligned}$$

$$\begin{aligned} \Psi_{ds} &= L_s I_{ds} + L_m I_{dr} \\ \Psi_{qs} &= L_s I_{qs} + L_m I_{qr} \quad (6) \\ \Psi_{dr} &= L_r I_{dr} + L_m I_{ds} \\ \Psi_{qr} &= L_r I_{qr} + L_m I_{qs} \quad (7) \end{aligned}$$

$$T_e = \frac{3}{2} n_p (\Psi_{ds} I_{qs} - \Psi_{qs} I_{ds}) \quad (8)$$

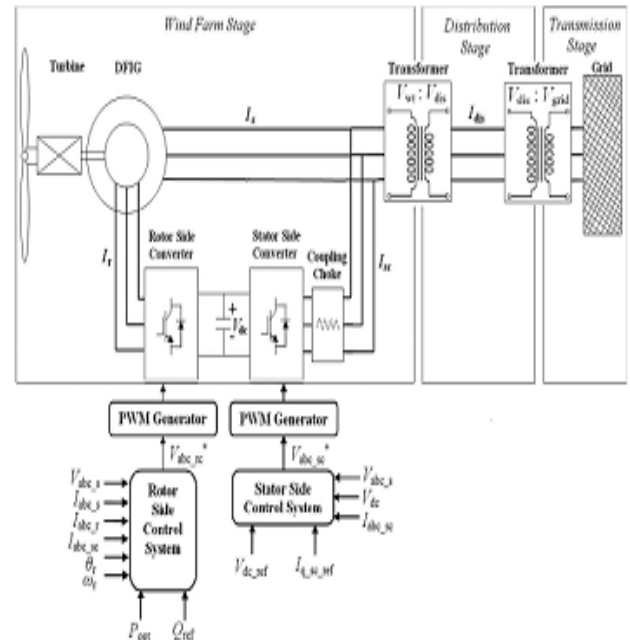


Fig. 7. Wind turbine–doubly fed induction generator system configuration.

A. Rotor-Side Converter Control

If the derivative parts in (5) are neglected, one can obtain stator flux as

Because of being directly connected to the grid, the stator voltage shares constant magnitude and frequency of the grid.

$$\begin{aligned} \Psi_{ds} &= (V_{qs} - R_s I_{qs}) / \omega_s \\ \Psi_{qs} &= (V_{ds} - R_s I_{ds}) / (-\omega_s) \\ \Psi_s &= \sqrt{\Psi_{ds}^2 + \Psi_{qs}^2} \quad (9) \end{aligned}$$

One could make the d-axis align with stator voltage vector; it is true that $V_s = V_{ds}$ and $V_{qs} = 0$, thus $\Psi_s = \Psi_{qs}$ and $\Psi_{ds} = 0$, which is of stator-voltage-oriented vector control scheme, as depicted in Fig. 8. According to (7)–(9), the rotor-side converter reference current is derived as

$$I_{dr_ref} = -\frac{2L_s T_e}{3n_p L_m \Psi_s} \quad (10)$$

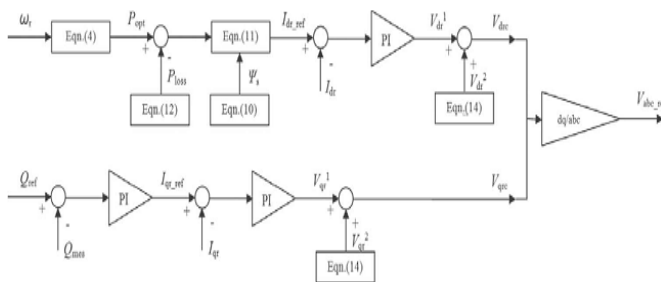


Fig. 10. Rotor-side converter control scheme

B. Stator-Side Converter Control

Concerning the use of three-phase series RL choke between stator- and stator-side converter, a cross-coupling model is required to derive the voltage signal of stator-side converter, as described in Fig. 11

$$V_{dsc} = V_{ds} - V_{dch}$$

$$V_{qsc} = V_{qs} - V_{qch} \quad (11)$$

The coupling part of voltage signals V_{dch}^2 and V_{qch}^2 is expressed as

$$V_{dch}^2 = R_c I_{dsc} - \omega_s L_c I_{qsc} \quad (12)$$

$$V_{qch}^2 = R_c I_{qsc} + \omega_s L_c I_{dsc} \quad (13)$$

the stator-side converter voltage signals V_{dsc} and V_{qsc} are obtained as follows and depicted in Fig. 11

$$V_{dsc} = V_{ds} - V_{dch}^1 - V_{dch}^2$$

$$V_{qsc} = V_{qs} - V_{qch}^1 - V_{qch}^2 \quad (14)$$

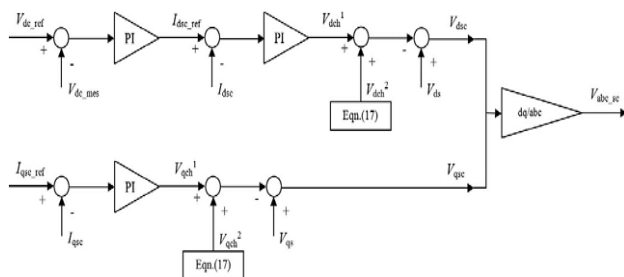


Fig. 11. Stator-side converter control scheme.

V. FUZZY LOGIC CONTROL

In FLC, basic control action is determined by a set of linguistic rules. These rules are determined by the system. Since the numerical variables are converted into linguistic variables, mathematical modeling of the

system is not required in FC. The FLC comprises of three parts: fuzzyfication, interference engine and defuzzyfication. The FC is characterized as; i.seven fuzzy sets for each input and output. ii.Triangular membership functions for simplicity. iii.Fuzzification using continuous universe of discourse. iv. Implication using Mamdani "s" „min“ operator. v. Defuzzification using the „height“ method..

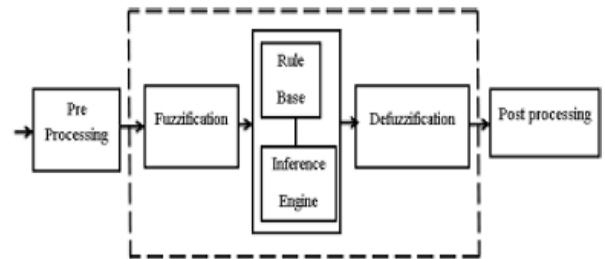


Fig 13.Fuzzy Logic Controller

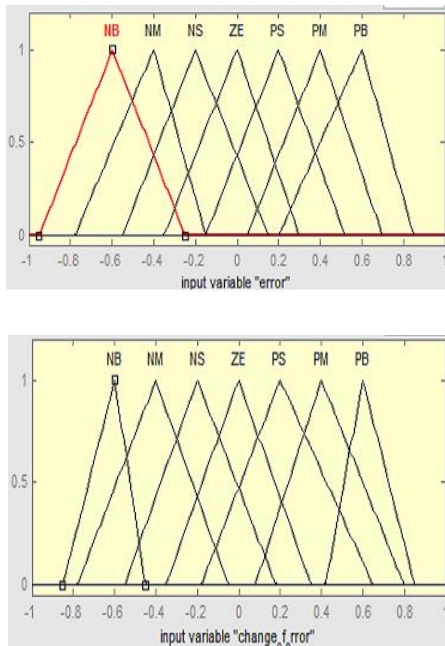
	NB	NM	NS	ZE	PS	PM	PB
NB	NB	NB	NB	NB	NM	NS	ZE
NM	NB	NB	NB	NM	NS	ZE	PS
NS	NB	NB	NM	NS	ZE	PS	PM
ZE	NB	NM	NS	ZE	PS	PM	PB
PS	NM	NS	ZE	PS	PM	PB	PB
PM	NS	ZE	PS	PM	PB	PB	PB
PB	ZE	PS	PM	PB	PB	PB	PB

FUZZY RULES

Fuzzification

Membership function values are assigned to the linguistic variables, using seven fuzzy subsets: NB (Negative Big),NM(Negative Medium), NS (Negative Small), ZE (Zero), PS (Positive Small),PM(Positive Medium) and PB (Positive Big). The partition of fuzzy subsets and the shape of membership function adapt the shape up to appropriate system. The value of input error $E(k)$ and change in error $CE(k)$ are normalized by an input scaling factor.

In this system the input scaling factor has been designed such that input values are between -1 and+1. The triangular shape of the membership function of this arrangement presumes that for any particular input there is only one dominant fuzzy subset.



Interference Method

Several composition methods such as Max–Min and Max-Dot have been proposed in the literature. In this paper Min method is used. The output membership function of each rule is given by the minimum operator and maximum operator. Table 1 shows rule base of the FLC Defuzzification

As a plant usually requires a non-fuzzy value of control, a defuzzification stage is needed. To compute the output of the FLC, „height“ method is used and the FLC output modifies the control output. Further, the output of FLC controls the switch in the inverter.. In order to control these parameters, they are sensed and compared with the reference values. To achieve this, the membership functions of FC are: error, change in error and output as shown in Figs.14(a), (b).

In the present work, for fuzzification, non-uniform fuzzifier has been used. If the exact values of error and change in error are small, they are divided conversely and if the values are large, they are divided coarsely. Where α is self-adjustable factor which can regulate the whole operation. E is the error of the system, C is the change in error and u is the control variable. A large value of error E indicates that given system is not

in the balanced state. If the system is unbalanced, the controller should enlarge its control variables to balance the system as early as possible. On the other hand, small value of the error E indicates that the system is near to balanced state. Overshoot plays an important role in the system stability.

Less overshoot is required for system stability and in restraining oscillations. C in (12) plays an important role, while the role of E is diminished. The optimization is done by α . The set of FC rules is made using Fig.14 is given in Table 1.

VI. SIMULATION RESULTS

Case i: By using PI controller

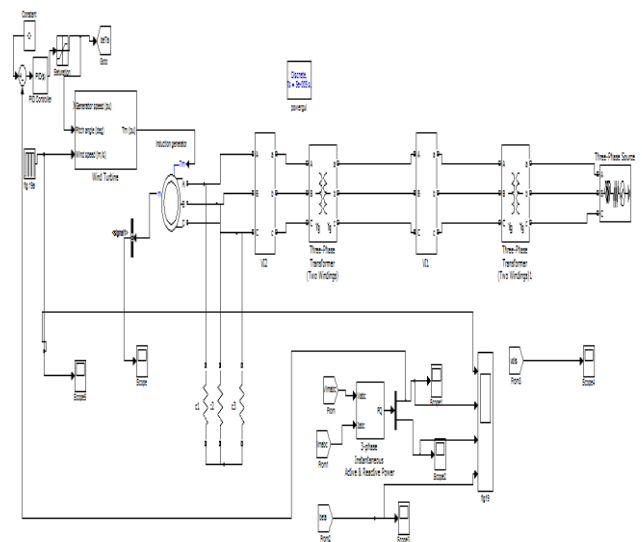


Fig.14. Simulink circuit for SCIG without STATCOM

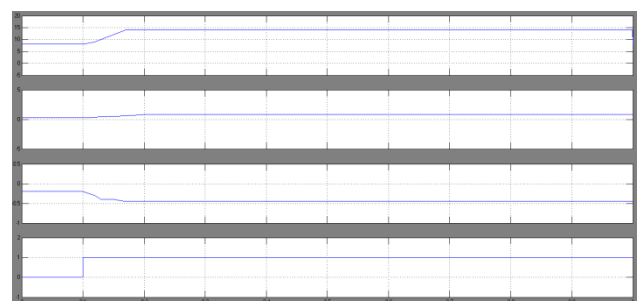


Fig. 15. Simulation results for SCIG system: (a) wind speed vw; (b) active power P; (c) reactive power Q; (d) pitch angle β .

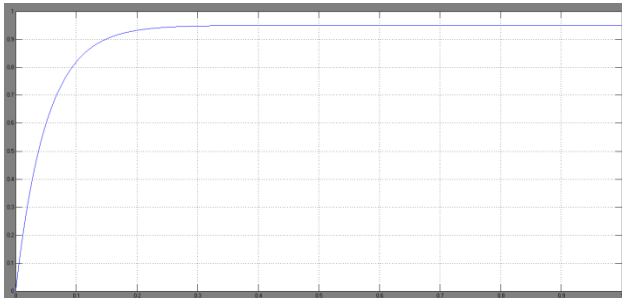


Fig.16. distribution voltage

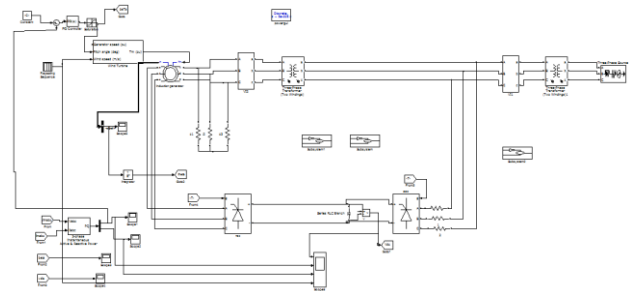


Fig.20. Simulink circuit for DFIG with STATCOM

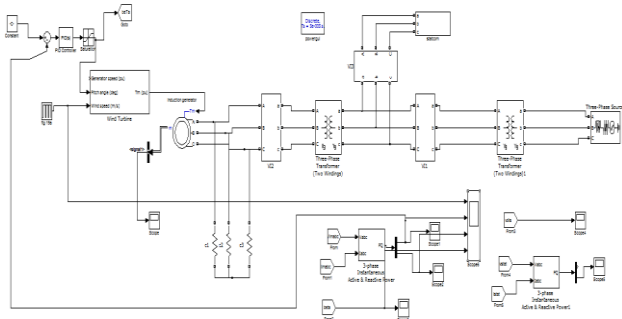


Fig.17. Simulink circuit for SCIG with STATCOM



Fig. 21. Simulation results for DFIG system: (a)dc link voltage (b) active power P; (c) reactive power Q; (d) wind speed

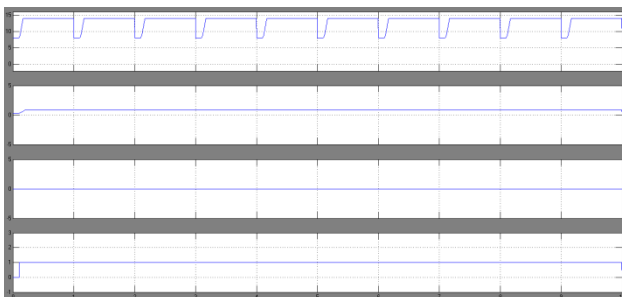


Fig. 18. Simulation results for SCIG system: (a) wind speed vw; (b) active power P; (c) reactive power Q; (d) pitch angle β .

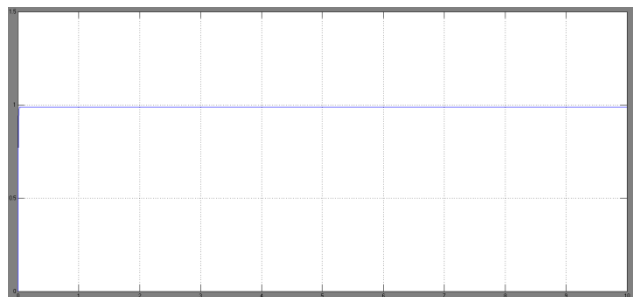


Fig.22. Simulation result for distribution voltage

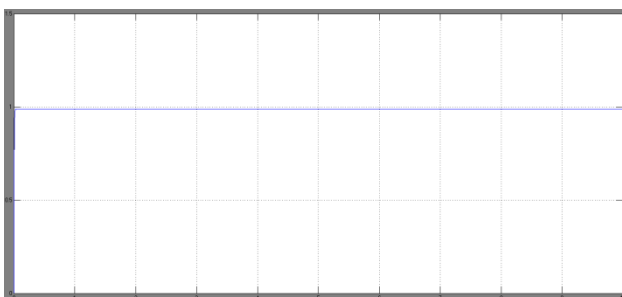


Fig.19. distribution voltage

Case ii: By using fuzzy controller

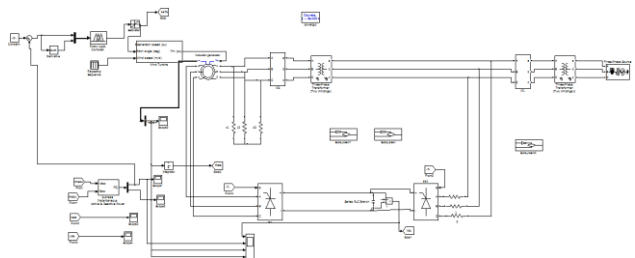


Fig.23. Simulink circuit for DFIG with statcom by fuzzy controller

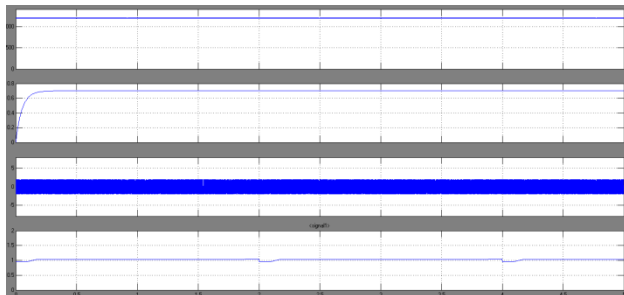


Fig. 24.. Simulation results for DFIG system: (a) wind speed v_w ; (b) active power P ; (c) reactive power Q ; (d) pitch angle β .

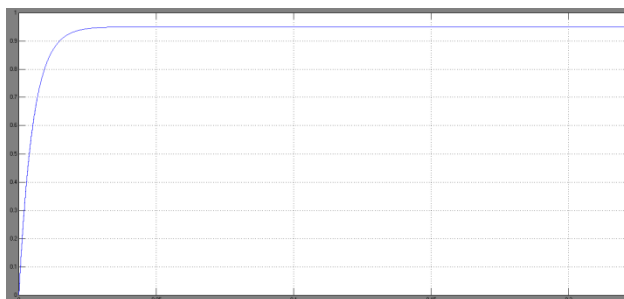


Fig.25. Simulation result for distributed voltage

VII. CONCLUSION

This paper proposes the performance comparison of fuzzy logic controlled wind power systems. This paper has presented the comparison of the wind turbine systems using SCIG and DFIG generator systems. A SCIG and a DFIG with fuzzy wind power systems are modelled and simulated in Mat lab/Simulink. The SCIG system presents the need of external reactive power source to support grid voltage, and it can keep the output power at the nominal level by pitch control but cannot accordingly change the rotor speed to achieve maximum wind power capture at different wind speeds. In contrast, the DFIG with fuzzy system does not need reactive power compensator to hold distribution line voltage and achieves optimal active power controlling. Both voltage control schemes for two converters consist of a current regulation part and a cross-coupling part. The turbine emulator system performs well and follows the theoretical and simulated maximum power extraction points in different operating conditions.

By using pi controller distributed voltage settling time is at 0.5 sec, but after using fuzzy controller the settling time is below 0.5 sec.

REFERENCES

- [1] M. Orabi, T. Ahmed, and M. Nakaoka, "Efficient performances of induction generator for wind energy utilization," in Proc. 30th Annu. Conf. IEEE Ind. Elect. Soc., Nov. 1704, pp. 838–843.
- [2] M. Molinas, J. A. Suul, and T. Undeland, "Low voltage ride through of wind farms with cage generators: STATCOM versus SVC," IEEE Trans. Power Electron., vol. 20, no. 3, pp. 1104–1117, May 1708.
- [3] Z. Chen, J. M. Guerrero, and F. Blaabjerg, "A review of the state of the art of power electronics for wind turbines," IEEE Trans. Power Electron., vol. 21, no. 8, pp. 1559–1575, Aug. 1709.
- [4] Y. Lei, A. Mullane, and G. Light body, "Modeling of the wind turbine with a doubly fed induction generator for grid integration studies," IEEE Trans. Energy Convers., vol. 18, no. 1, pp. 257–264, Mar. 1706. IEEE Int. Conf. Mechatron. Autom., Aug. 1709, pp. 1976
- [5] R. Ganon, G. Sybille, and S. Bernard, "Modeling and real-time simulation of a doubly-fed induction generator driven by a wind turbine," presented at the Int. Conf. Power Systems Transients, Montreal, QC, Canada, Jun. 1705, Paper IPST05-162.
- [6] H. Sun, Y. Ren, and H. Li, "DFIG wind power generation based on back-to-back PWM converter," in Proc.
- [7] L. Xu and P. Cartwright, "Direct active and reactive power control of DFIG for wind energy generation," IEEE Trans. Energy Convers., vol. 18, no. 3, pp. 750–758, Sep. 1706.



[8] S. Heier, *Grid Integration of Wind Energy Conversion Systems*. Hoboken, NJ, USA: Wiley, 1706.

[9] N. W. Miller, W. W. Price, and J. J. Sanchez-Gasca, "Dynamic modeling of GE 1.5 And 3.6 wind turbine generators," *GE Power Systems Energy Consulting, Gen. Elect. Int., Inc., Schenectady, NY, USA, Oct. 1703*.

[10] R. Pena, J. C. Clare, and G. M. Asher, "Doubly fed induction generator using back-to-back PWM converters and its application to variable-speed wind-energy generation," *Proc. Inst. Elect. Eng.—Elect. Power Appl.*, vol. 143, no. 3, pp. 201–211, May 1696.

[11] Feijoo, J. Cidras, and C. Carrillo, "Third order model for the doubly-fed induction machine," *Elect. Power Syst. Res.*, vol. 56, no. 2, pp. 118–127, Nov. 1700.

[12] T. Ghennam, E. M. Berkouk, and B. Francois, "DC-link voltage balancing algorithm using a space-vector hysteresis current control for three-level VSI applied for wind conversion system," in *Proc. Power Elect. Appl. Eur. Conf.*, Sep. 1707, pp. 1–10.

[13] M. Stiebler, *Wind Energy Systems for Electric Power Generation*. Berlin, Germany: Springer-Verlag, 1708.